Journal of Photochemistry and Photobiology A: Chemistry 230 (2012) 38–46

Contents lists available at SciVerse ScienceDirect

Journal of Photochemistry and Photobiology A: Chemistry

journal homepage: www.elsevier.com/locate/jphotochem

Photophysical properties and photostability of novel unsymmetric polycyclicphenazine-type D-π-A fluorescent dyes and the dye-doped films

Haruka Egawa Ooyama*, Akiko Hayashi, Toshiki Mamura, Takashi Ide, Toshihiko Hino, Takuya Tanigami, Katsuhira Yoshida*

Department of Applied Science, Graduate School of Integrated Arts and Science, Kochi University, Akebono-cho, Kochi 780-8520, Japan

ARTICLE INFO

Article history:
Received 17 June 2011
Received in revised form 1 December 2011
Accepted 14 December 2011
Available online 27 December 2011

Keywords:
Fluorescent dye
Photophysical property
Photostability
Fluorescent polymer film
Wavelength conversion

ABSTRACT

Structural isomers of unsymmetric polycyclicphenazine-type D-π-A fluorescent dyes have been newly synthesized and characterized in both solution and polymer films. The dyes exhibited two strong absorption bands at around 328–401 nm and 516–532 nm, and an intense fluorescence band at around 595–629 nm (Φ = 0.32–0.84) in 1,4-dioxane. The dye-doped polymer films showed good ability of wavelength conversion; the films can efficiently convert ultraviolet and green-yellow lights into red light (Φ = 0.43–0.86). Moreover, the photostability of the dyes-doped PS, PMMA, and PLA films has been investigated.

1. Introduction

Photosynthesis and photomorphogenesis in plant growth are significantly controlled by light quality. In general, many kinds of wavelength conversion films such as UV, visible and near-infrared light absorbing films have been used for various regulations of plant growth [1–5]. It is known that red and blue light efficiently promotes the plant growth in many kinds of plants [6–8]. However, there are few reports on fluorescent dye-doped films evaluated as wavelength conversion films [9,10]. For the polymer films, it is required to enhance red light without decrease of blue light of light source such as the sun light. To develop the fluorescent dyes which satisfy the above requisition, we have performed the semi-empirical molecular orbital calculations (AM1 and INDO/S) and estimated approximately the absorption wavelengths of the dye molecules. In this study, we have designed and synthesized novel unsymmetric polycyclic phenazine-type D-π-A fluorescent dyes **3a**, **3b**, and **6a**, **6b** which are structural isomers. The photophysical properties, photostability and the wavelength conversion ability of the dyes in both solution and polymer films have also been investigated.

2. Result and discussion

2.1. Semi-empirical MO calculations (AM1, INDO/S)

We have carried out semi-empirical molecular orbital (MO) calculations for the designed fluorophores **3** and **6** to elucidate the difference of photophysical properties. The structures of these compounds were optimized by MOPAC/AM1 [12] and then the electron transition spectra were calculated by the INDO/S [13–15]. The calculated first and second absorption wavelengths and the transition character of the bands are collected in Table 1. The change of electron density accompanying the first electronic excitation (HOMO → LUMO) is shown in Fig. 1, which reveals the migration of intramolecular charge transfer from the dibutylamino groups as a donor to the pyrazine ring with a butoxy carbonyl group as an acceptor. The calculated absorption wavelengths of **3a** (430 nm, f = 0.63) and **3b** (432 nm, f = 0.47), which have benzofuran skeleton, were longer than those of **6a** (420 nm, f = 0.87) and **6b** (422 nm, f = 0.71), which have benzopyran skeleton. Moreover, the oscillator strength of the fluorophores, which have benzopyrane skeleton, was larger than those of the fluorophores, which have benzofuran skeleton. The second absorption maxima were predicted to be appeared at around 330 nm for **3a** and **3b** and at around 355 nm for **6a** and **6b**. It is known that the absorption wavelengths of INDO/S calculations are blue-shifted by ca. 50–120 nm than the experimental values [16,17]. Therefore, we expected that the fluorophores **3** and **6** could convert green-yellow lights into red light.

* Corresponding authors. Tel.: +81 88 844 8296; fax: +81 88 844 8359.
E-mail address: kyoshida@kochi-u.ac.jp (K. Yoshida).

1010-6030/$ – see front matter © 2011 Elsevier B.V. All rights reserved.
doi:10.1016/j.jphotochem.2011.12.009

Table 1
Calculated absorption spectra for the fluorescent dyes **3** and **6**.

Dye	μ [D][a]	Absorption (calc.)		CI component[c]	$\Delta\mu$ [D][d]
		λ_{max} (nm)	f[b]		
3a	5.75	430	0.63	HOMO → LUMO (83%)	10.21
		329	0.76	HOMO-1 → LUMO (34%)	
				HOMO → LUMO + 1 (22%)	
				HOMO → LUMO + 5 (10%)	
				HOMO → LUMO + 2 (8%)	
				HOMO → LUMO + 4 (4%)	
3b	6.64	432	0.47	HOMO → LUMO (81%)	9.92
		331	1.01	HOMO-1 → LUMO (42%)	
				HOMO → LUMO + 1 (20%)	
				HOMO → LUMO + 5 (7%)	
				HOMO → LUMO + 2 (6%)	
				HOMO → LUMO + 4 (5%)	
6a	6.16	420	0.87	HOMO → LUMO (80%)	7.86
		357	0.17	HOMO → LUMO + 1 (38%)	
				HOMO-2 → LUMO (27%)	
				HOMO-1 → LUMO (11%)	
				HOMO → LUMO (5%)	
6b	6.77	422	0.71	HOMO → LUMO (80%)	7.81
		353	0.23	HOMO → LUMO + 1 (49%)	
				HOMO-2 → LUMO (17%)	
				HOMO-1 → LUMO (8%)	
				HOMO → LUMO + 2 (4%)	
				HOMO-3 → LUMO (3%)	

[a] The values of the dipole moment in the ground state.
[b] Oscillator strength.
[c] The transition is shown by an arrow from one orbital to another, followed by its percentage CI (configuration interaction) component.
[d] The difference in dipole moment between the excited and the ground states.

2.2. Synthesis of the unsymmetric polycyclic phenazine-type D-π-A fluorescent dyes

The synthesis of the unsymmetric isomeric phenazine-type D-π-A fluorescent dyes **3a**, **3b**, **6a** and **6b** is shown in Schemes 1 and 2. We used polycyclic *o*-quinone derivatives **1** and **4** as starting materials [18]. The reaction of the polycyclic *o*-quinones **1** and **4** with 3,4-diaminobenzoic acid produced the intermediates **2a**, **2b**, **4a** and **4b**, which are structural isomers having polycyclicphenazine skeleton, respectively. The esterification of the intermediates produced the fluorescent dyes, **3a**, **3b**, **6a** and **6b** in 44%, 46%, 16% and 73%, respectively. These compounds were completely characterized by ^{1}H NMR, IR, and elemental analysis. A comparison of the observed and calculated UV–VIS spectra for the compounds **3a**, **3b**, **6a** and **6b** and the X-ray crystal analysis of **3a** were performed for identification of their structures, which will be described later on.

2.3. Spectroscopic properties of the polycyclic phenazine-type D-π-A fluorescent dyes in solution

The absorption and fluorescence spectra of **3a**, **3b**, **6a** and **6b** were measured in 1,4-dioxane, THF, and DMSO. The absorption and fluorescence spectra in 1,4-dioxane are shown in Figs. 2 and 3 as an example and all the spectroscopic data are summarized in Table 2. The shapes of the absorption spectra in solution were comparatively good agreement with the MO calculation data shown in Table 1. The substituent-isomers **3a** and **3b** which have a benzofuran skeleton exhibited two absorption maxima at around 517 nm and 350–390 nm and the fluorescence band appeared at around 625 nm in 1,4-dioxane. The wavelengths of the absorption and fluorescence maxima between the substituent-isomers were almost same, however, the fluorescence quantum yield of **3a** (Φ = 0.69) was higher than that of **3b** (Φ = 0.36). Similar relation was also

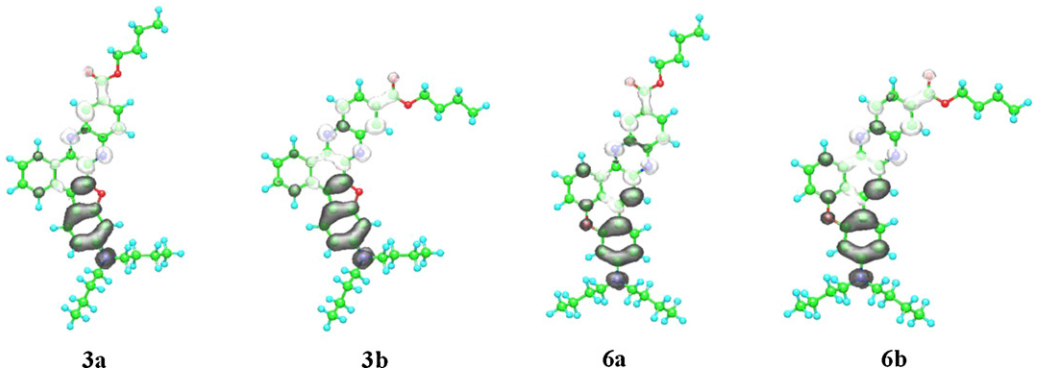

Fig. 1. Calculated changes in electron density accompanying the first electronic excitation of **3a**, **3b**, **6a** and **6b**. The black and white lobes signify degreases and increase in electron density accompanying the electronic transition, respectively. Their areas indicate the magnitude of the electron density change.

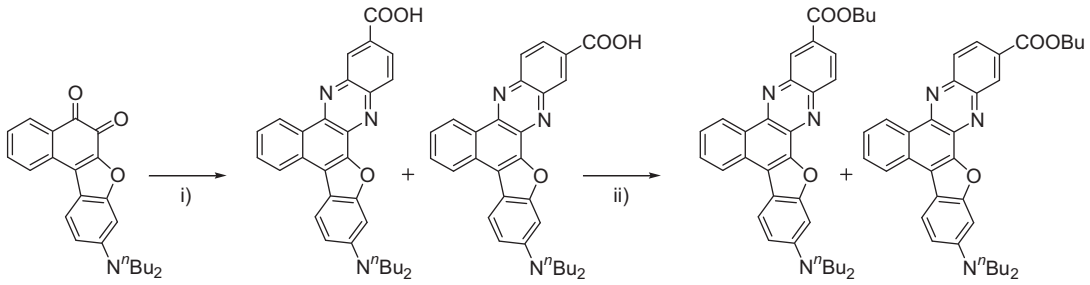

Scheme 1. Synthesis of the unsymmetric phenazine-type D-π-A fluorescent dyes **3a** and **3b**. (i) 3,4-Diaminobenzoic acid, acetic acid, 110 °C, 1.5 h; (ii) ^{n}BuI, Na_2CO_3, DMF, 110 °C, 2 h, 44% for **3a**, 46% for **3b**.

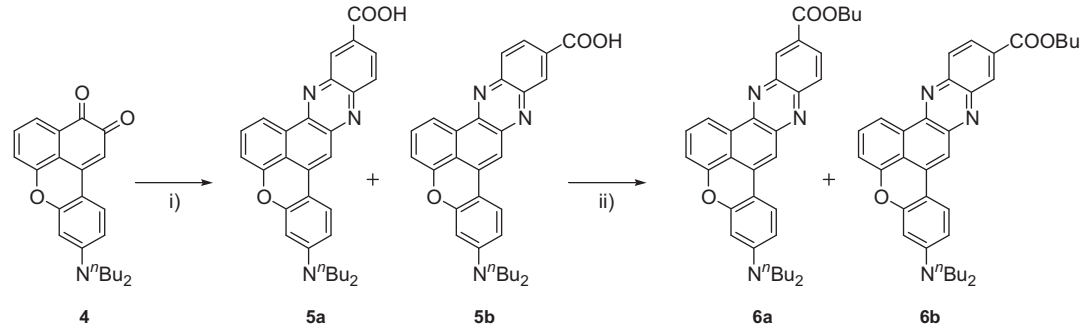

Scheme 2. Synthesis of the unsymmetric phenazine-type D-π-A fluorescent dyes **6a** and **6b**. (i) 3,4-Diaminobenzoic acid, acetic acid, 110 °C, 1.5 h; (ii) ^{n}BuI, Na_2CO_3, DMF, 110 °C, 2 h, 16% for **6a**, 73% for **6b**.

observed between the substituent-isomers **6a** and **6b**, which have a benzopyrane skeleton. In addition, a remarkable solvent effect was observed. In contrast to the absorption wavelength the fluorescence wavelength showed much larger bathochromic shift with increasing solvent polarity. This behavior is known as typical of CT-type emission originating from the excited state. Moreover, comparing the structure-isomers between **3** and **6**, it was found that the dyes **6a** and **6b** have larger absorption coefficients than the dyes **3a** and **3b**, which was compatible with the MO calculation that the oscillator strength of **6** (f = 0.71–0.87) is larger than that of **3** (f = 0.47-0.63).

A significant difference was also observed in the Stokes shifts between the structure-isomers **3** and **6**: the isomers **3a** and **3b** showed larger stokes shift values than the isomers **6a** and **6b**. The larger stokes values of **3a** and **3b** compared to those of **6a** and **6b** could be interpreted by the difference in their dipole moment in the excited state. From the calculated results, the dyes **3a** and **3b** have larger dipole moment in the excited state than **6a** and **6b**. Therefore, the excited state of the dyes **3a** and **3b** was more stabilized by electrostatic interaction with solvent molecules.

2.4. Spectroscopic properties of the polycyclicphenazine-type D-π-A fluorescent dyes in polymer films

The absorption and fluorescence properties of the isomeric dyes **3a**, **3b**, **6a** and **6b** in polymer films were investigated. Polylactic acid (PLA), polymethylmethacrylate (PMMA) and polystyrene (PS) were used as polymer substrates. The dye-doped polymer

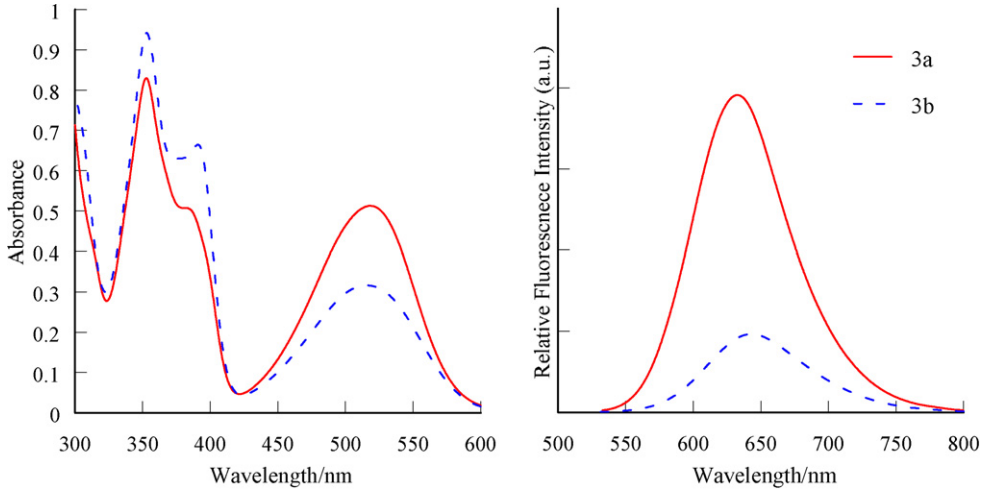

Fig. 2. Absorption and fluorescence spectra of **3a** and **3b** in 1,4-dioxane.

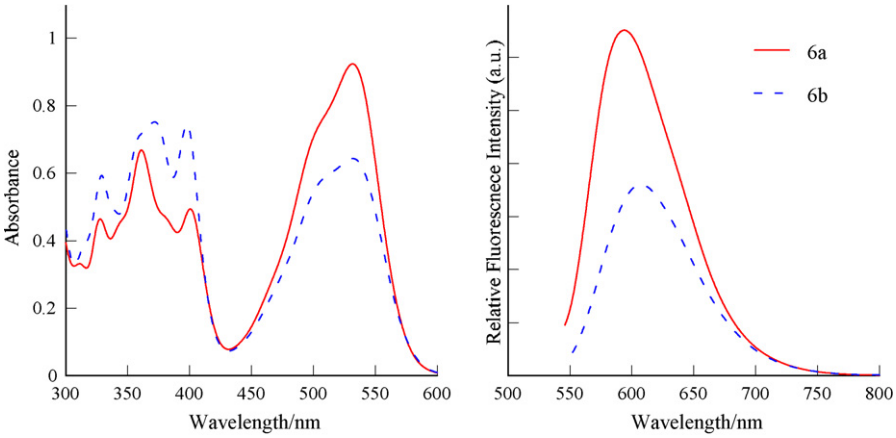

Fig. 3. Absorption and fluorescence spectra of **6a** and **6b** in 1,4-dioxane.

Table 2
Spectroscopic properties of the fluorescent dyes in solution.

Dye	Solvent	Absorption λ_{max} (nm)[a] (ε_{max}/dm^3 mol^{-1} cm^{-1})	Fluorescence λ_{max} (nm)[b] (Φ[c])	SS[d] $\Delta\lambda_{max}$ (nm)
3a	1,4-Dioxane	518 (24,800), 390[sh], 353 (39,600)	620 (0.69)	102
	THF	527 (30,800), 400[sh], 355(49,600)	660 (0.32)	133
	DMSO	542 (19,600), 400[sh], 361 (32,000)	732 (0.02)	190
3b	1,4-Dioxane	516 (16,400), 390 (32,400), 353 (46,000)	629 (0.36)	113
	THF	524 (21,600), 393 (44,400), 355 (62,400)	671 (0.06)	147
	DMSO	540(13,000), 398[sh] (24,900), 360 (36,400)	–[e]	–
6a	1,4-Dioxane	532 (39,400), 401 (20,800), 361 (28,500), 328 (20,100)	595(0.84)	63
	THF	537 (36,500), 402 (20,300), 362 (26,000), 329 (17,900)	629(0.75)	92
	DMSO	547 (27,500), 406 (15,700), 367 (19,300), 328 (12,700)	688(0.15)	147
6b	1,4-Dioxane	531 (26,100), 397 (29,700), 372 (30,000), 328 (23,700)	607(0.75)	76
	THF	536 (25,400), 400 (29,200), 372 (29,100), 329 (22,800)	637(0.44)	101
	DMSO	546 (23,400), 404 (26,800), 378 (24,800), 334(19,700)	701(0.02)	155

[a] $c = 2.5 \times 10^{-5}$ M.
[b] $c = 2.5 \times 10^{-6}$ M.
[c] The Φ value was determined with a calibrated integrating sphere system.
[d] Stokes shift value.
[e] Non emission peak.

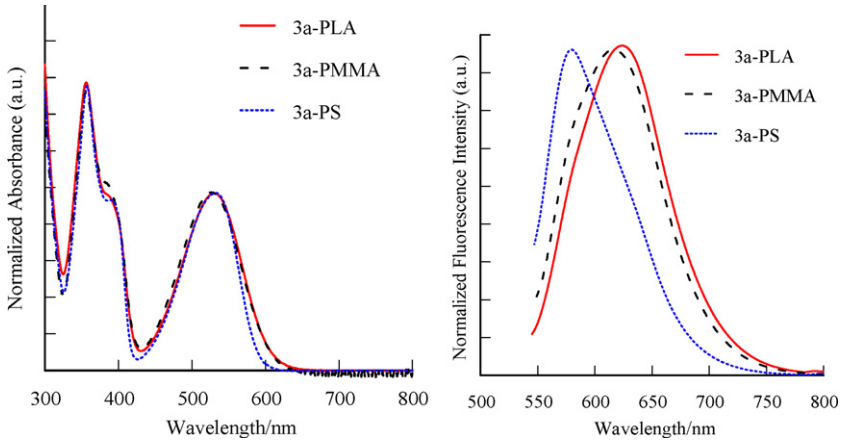

Fig. 4. Normalized absorption and fluorescence spectra of **3a** in polymer thin films.

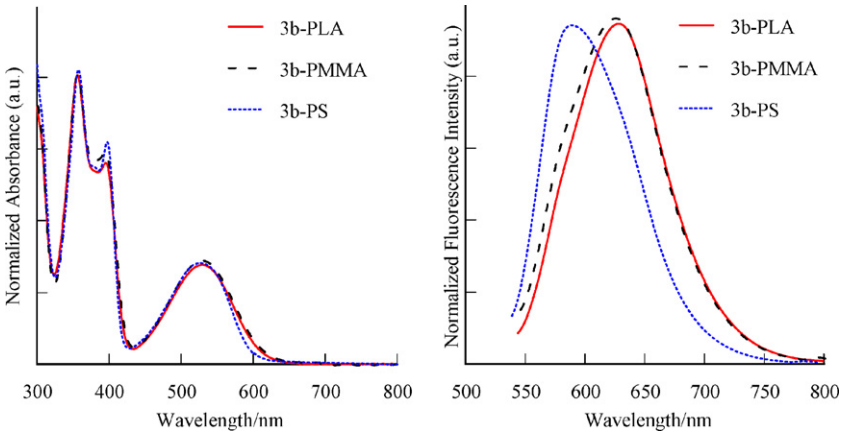

Fig. 5. Normalized absorption and fluorescence spectra of **3b** in polymer thin films.

films were prepared by casting a polymer solution containing a fluorescent dye on a cover glass. The polymer solution was prepared by dissolving the fluorescent dye and polymer resin pellets in dichloromethane. The concentration of the fluorescent dye was 0.05 wt.% and the thickness of the films was ca. 100 μm. As examples, the absorption and fluorescent spectra of the dye (**3a** and **3b)** doped PLA-, PMMA-, and PS-films are shown in Figs. 4 and 5, and the spectroscopic data are summarized in Table 3.

The dye (**3a** and **3b**) doped polymer thin films showed the absorption band at around 529–535 nm and 527–530 nm and the fluorescence band appeared at around 572–598 nm (Φ = 0.74–0.86) and 570–600 nm (Φ = 0.48–0.78), respectively. On the other hand, the dye (**6a** and **6b**) doped polymer thin films showed the absorption band at around 539–543 nm and 537–545 nm and the fluorescence band appeared at around 570–587 nm (Φ = 0.71–0.79) and 572–607 nm (Φ = 0.43–0.76), respectively. Above data show that the absorption wavelengths are not affected by the substrate of polymer, but the emission wavelengths are considerably changed. It was suggested that the emission peak tends to be red-shifted with increase in the relative dielectric constant (ε_r) of polymers; PS (ε_r = 2.42) < PLA (ε_r = 2.56) < PMMA (ε_r = 2.76). The dyes in PS film exhibited higher quantum yield than those in the other polymer films.

Table 3
Absorption and fluorescence spectral data of **3a**, **3b**, **6a** and **6b** in polymer thin films.

Dye	Polymer	Absorption, λ_{max} (nm)	Fluorescence, λ_{max} (nm) (Φ^a)	SS^b $\Delta\lambda_{max}$ (nm)
3a	PLA	529, 400, 357	585 (–)	56
	PMMA	535, 349	598 (0.74)	63
	PS	534, 400, 358	572 (0.86)	38
3b	PLA	530, 400, 357	600 (–)	70
	PMMA	527, 400, 357	588 (0.48)	61
	PS	528, 400, 358	570 (0.78)	42
6a	PLA	539, 400, 364	587 (–)	48
	PMMA	543, 400, 364	586 (0.71)	43
	PS	542, 400, 365	570 (0.79)	28
6b	PLA	537, 400, 371	607 (–)	70
	PMMA	541, 400, 361	598 (0.43)	57
	PS	545, 400, 377	572 (0.76)	27

[a] The Φ value was determined with a calibrated integrating sphere system.
[b] Stokes shift value.

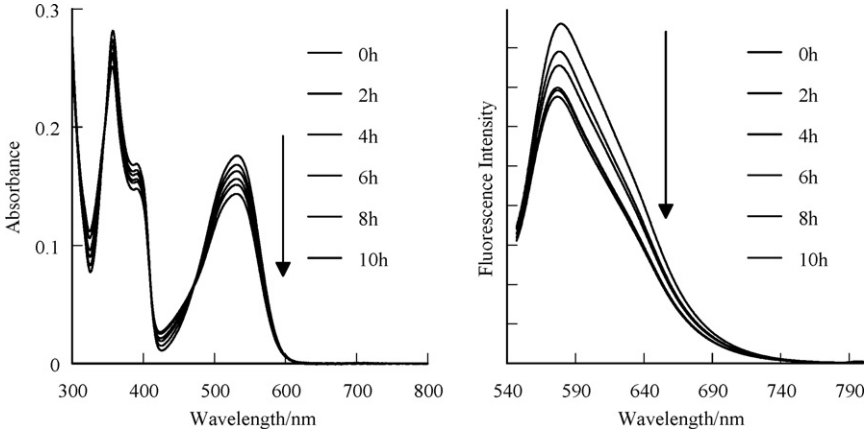

Fig. 6. Absorption (left) and fluorescence (right) spectral changes of **3a** in PS film.

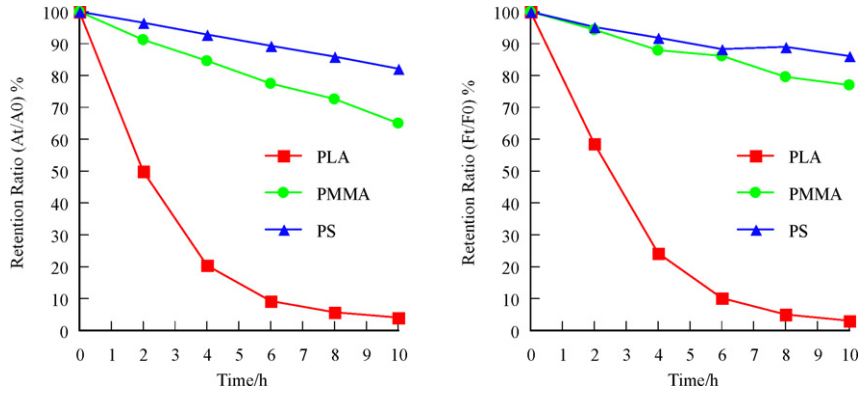

Fig. 7. Absorption (left) and fluorescence (right) retention ratio of **3a** in polymer films.

2.5. Photostabilities of the polycyclicphenazine-type D-π-A fluorescent dyes in polymer films

Photostability of the dye-doped polymer films were investigated by irradiating visible region light (300–800 nm) on the polymer films with a xenone accelerated weathering tester (Q-Sun Xe-1). The obtained data of photostability are summarized in Table 4. As an example, the absorption and fluorescence spectral changes of the **3a**-doped PS film upon photoirradiation are shown in Fig. 6. The maximum absorbance at 534 nm and the maximum fluorescence at 572 nm were gradually decreased. Figs. 7 and 8 show the plot of the absorption and fluorescence retention ratios vs. time in the photofading process of the dyes **3a** and **3b** in polymer films. The retention ratios were calculated by the following equation;

$$\frac{A_t \text{ or } F_t}{A_0 \text{ or } F_0} \times 100 = \text{Retention ratio (\%)}$$

A_0, F_0 = Initial maximum absorbance or fluorescence intensity at 0 h

A_t, F_t = Maximum absorbance or fluorescence intensity after t hours irradiation

Table 4
Absorption and fluorescence retention ratio of the phenazine-type fluorescent dyes in polymer films.

Compound	Medium	Retention ratio (%) After 10 h	
		Abs.	Flu.
3a	PLA	4	3
	PMMA	65	77
	PS	82	86
3b	PLA	3	2
	PMMA	6	8
	PS	76	81
6a	PLA	4	5
	PMMA	62	89
	PS	82	82
6b	PLA	5	4
	PMMA	55	67
	PS	75	84

It was found that the photofading rate was considerably dependent on the polymer substrates; the absorption and fluorescence retention ratios of the dye-doped PS films were higher than those of the dye-doped PMMA and PLA films. The similar phenomena were observed in the previous paper [19]. In addition, comparing the retention ratio of the fluorescent dyes **3a**, **3b**, **6a** and **6b** in PMMA films, the photosatability increased in the order of **3b** < **6b** < **3a** < **6a**. It seemed that the dye-doped films exhibiting higher florescence quantum yield tended to show better photostability. Thus, it was suggested that the photostability of the dye-doped polymer films are affected not only by the natures of polymer substrate but also by the skeleton and/or substituent position of dye. Therefore, the combination of the fluorescent dye and polymer substrate is also very important for photostabilization of dye-doped films.

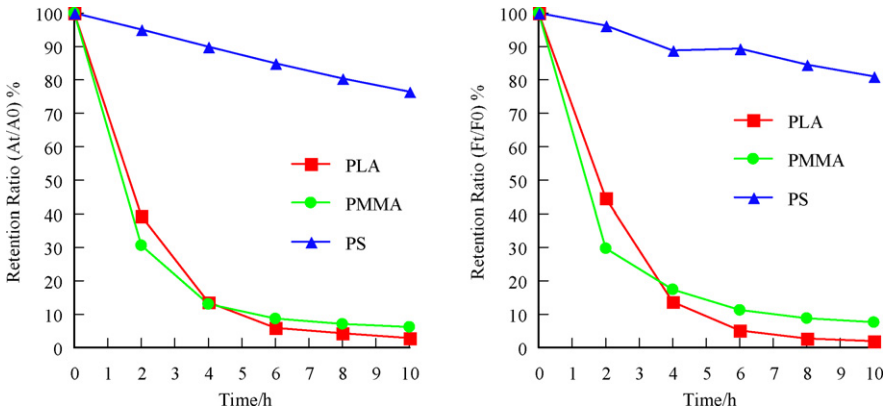

Fig. 8. Absorption (left) and fluorescence (right) retention ratio of **3b** in polymer films.

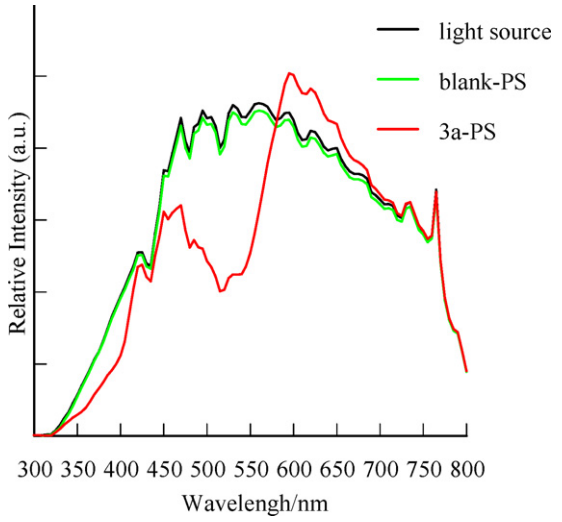

Fig. 9. Wavelength distribution spectra of the light source, blank-PS and **3a**-doped PS films.

2.6. Wavelength conversion function of the dye-doped polymer films

Wavelength conversion ability of the **3a**-doped PS film, which exhibited better photophysical properties and photostability than the other dyes, has been investigated. The ability of wavelength conversion was measured by using a flash multi photometry system (MCPD-3000, Ootsuka Electronics Co., Ltd.) and the pseudo-sunlight (HAL-302, Asahi Spectra Co., Ltd.) as a light source. Fig. 9 shows wavelength distribution spectra of the light source, PS film without dye as blank, and the **3a**-doped PS film. Comparing the three wavelength distribution curves, it was found that the **3a**-doped PS film absorbs UV and green-yellow lights and increases red light. As a result, the **3a**-doped PS film exhibited good wavelength conversion ability. Moreover, we have found that such a red fluorescent film can increase the PLB proliferation of *Cymbidium finlaysonianum*, even if the film is covered only during early stage of the culture [8,11].

3. Conclusion

We have designed and synthesized novel polycyclic phenazine-type fluorescent dyes **3a**, **3b**, **6a** and **6b**, which are structural isomers. These dyes exhibited two strong absorption bands at around 328–401 nm and 516–532 nm and a fluorescence band (Φ = 0.32–0.84) at around 595–629 nm in 1,4-dioxane. A remarkable solvent effect was observed and the fluorescence wavelength of the dyes was largely red-shifted with increasing solvent polarity. Moreover, we have investigated the photophysical properties and photostability of the fluorescent dyes in polymer films (PMMA, PLA, PS). The **3a**-, **6a**-, and **6b**-doped PS films exhibited a good wavelength conversion ability, which efficiently convert ultraviolet and green-yellow lights into red light (Φ = 0.71–0.86), and good photostability.

4. Experimental

4.1. General

Melting points were determined on Rigaku Thermo Pulus 2 system TG8120. IR spectra were recorded on a JASCO FT/IR-5300 spectrometer for sample in KBr pellet form. Absorption spectra were observed with a JASCO UV-670 spectrophotometer and fluorescence spectra were measured with a JASCO FP-6600 spectrophotometer. The fluorescence quantum yields (Φ) of solutions and the dye-doped polymer films were determined by a Hamamatsu C9920-12 by using a calibrated integrating sphere. The ability of wavelength conversion was measured by using a flash multi photometry system (MCPD-3000, Ootsuka Electronics Co., Ltd.) and a pseudo-sunlight (HAL-302, Asahi Spectra Co., Ltd.). Elemental analyses were recorded on a Perkin Elmer 2400 II CHN analyzer. ^{1}H NMR spectra were recorded on a JNM-LA-400 (400 MHz) FT NMR spectrometer with tetramethylsilane (TMS) as an internal standard. Column chromatography was performed on silica gel (KANTO CHEMICAL, 60N, spherical, neutral).

4.2. Synthesis

Synthesis of the mixture of 2-dibutylamino-15-oxa-9,14-diaza-indeno[2,1-a]-benzo [c]-anthracene-11-carboxylic acid (2a) and 2-dibutylamino-15-oxa-9,14-diaza indeno[2,1-a]-benzo[c]anthracene-12-carboxylic acid (2b). A solution of polycyclic *o*-quinone **1** (5.00 g, 13.30 mmol) and 3,4-diamino benzoic acid (2.02 g, 13.30 mmol) in acetic acid was stirred at 110 °C for 1.5 h. After the reaction, the reaction mixture was poured into cold water. The resulting precipitate was filtered and the residue was washed with small amount of CH_2Cl_2 and then dried to give a mixture of **2a** and **2b** (6.13 g, 94% yield) as red powder.

Synthesis of 2-dibutylamino-15-oxa-9,14-diaza-indeno[2,1-a]benzo[c]anthracene-11-carboxylic butylester (3a) and 2-dibutylamino-15-oxa-9,14-diaza-indeno[2,1-a] benzo[c]-anthracene-12-carboxylic butyl ester (3b)

A solution of the mixture of **2a** and **2b** (1.00 g, 2.03 mmol), 1-iodobutane (0.70 g, 3.81 mmol) and Na_2CO_3 (0.51 g, 4.82 mmol) in DMF was stirred at 110 °C for 2 h. After the reaction, the reaction mixture was extracted with CH_2Cl_2 and washed with water. The combined organic layer was evaporated and the residue was chromatographed on silica (CH_2Cl_2 as eluent) to give **3a** (0.48 g, 44% yield) as red powder and **3b** (0.50 g, 46% yield) as red powder.

Compound **3a**: mp.159 °C; IR(KBr)/cm^{-1}: 1713; ^{1}H-NMR ($CDCl_3$) δ = 1.00–1.07 (m, 9H), 1.44 (qt, J = 6.84, 7.80 Hz, 4H), 1.54–1.64 (m, 2H), 1.69 (tt, J = 6.84, 7.80 Hz, 4H), 1.87 (tt, J = 6.84, 7.80 Hz, 2H), 3.41 (t, J = 7.80 Hz, 4H), 4.46 (t, J = 6.84 Hz, 2H), 6.86 (d, J = 6.84 Hz, 1H), 7.03 (s, 1H) 7.77 (dd, J = 6.80, 7.84 Hz, 1H), 7.88 (dd, J = 6.84, 7.80 Hz, 1H), 8.43 (s, 2H), 8.50 (d, J = 7.84 Hz, 1H), 9.04 (s, 1H), 9.47 (d, J = 7.80 Hz, 1H); elemental analysis calcd (%) for $C_{35}H_{37}N_3O_3$: C 76.75, H 6.81, N 7.67; found; C 77.05, H 6.82, N 7.75.

Compound **3b**: mp.198 °C; IR(KBr)/cm^{-1}: 1718; ^{1}H-NMR ($CDCl_3$) δ = 1.00–1.07 (m, 9H), 1.44 (qt, J = 6.84, 7.80 Hz, 4H), 1.52–1.63 (m, 2H), 1.69 (tt, J = 6.84, 7.80 Hz, 4H), 1.84 (tt, J = 6.84, 7.80 Hz, 2H), 3.42(t, J = 7.80 Hz, 4H), 4.45 (t, J = 6.84 Hz, 2H), 6.87 (dd, J = 1.96, 8.80 Hz, 1H), 7.06 (d, J = 1.96 Hz, 1H), 7.77 (dd, J = 6.84, 7.80 Hz, 1H) 7.90 (dd, J = 6.84, 7.80 Hz, 1H), 8.13 (d, J = 9.76 Hz, 1H), 8.36–8.43 (m, 2H), 8.51 (d, J = 7.84 Hz, 1H), 9.17 (s, 1H), 9.48 (d, J = 7.84 Hz, 1H); elemental analysis calcd (%) for $C_{35}H_{37}N_3O_3$: C 76.75, H 6.81, N 7.67; found; C 76.69, H 6.82, N 7.70.

Synthesis of the mixture of 6-dibutylamino-4-oxa-10,15-diaza-dibenzo[a,de] naphthacene-13-carboxylic acid (5a) and 6-dibutylamino-4-oxa-10,15-diaza-dibenzo[a,de]naphthacene-12-carboxylic acid (5b)

A solution of polycyclic *o*-quinone **4** (2.00 g, 5.33 mmol) and 3,4-diamino benzoic acid (0.81 g, 5.33 mmol) in acetic acid was stirred at 110 °C for 1.5 h. After the reaction, the reaction mixture was poured into cold water. The resulting precipitate was filtered and the residue was washed with small amount of CH_2Cl_2 and then dried to give a mixture of **5a** and **5b** (2.38 g, 91% yield) as red powder.

Synthesis of 6-dibutylamino-4-oxa-10,15-diaza-dibenzo [a,de]naphthacene-13-carboxylic butyl ester (6a) and 6-dibutylamino-4-oxa-10,15-diaza-dibenzo[a,de] naphthacene-12-carboxylic butyl ester (6b)

A solution of the mixture of **6a** and **6b** (2.00 g, 4.07 mmol), 1-iodobutane (1.40 g, 7.63 mmol) and Na_2CO_3 (0.51 g, 4.82 mmol) in DMF was stirred at 110 °C for 2 h. After the reaction, the reaction mixture was extracted with CH_2Cl_2 and washed with water. The combined organic layer was evaporate and the residue was chromatographed on silica (CH_2Cl_2 as eluent) to give **6a** (0.35 g, 16% yield) as red powder and **6b** (1.65 g, 73% yield) as red powder.

Compound **6a**: mp.149 °C; IR(KBr)/cm^{-1}: 1712; ^{1}H-NMR ($CDCl_3$) δ = 1.01 (t, J = 7.32 Hz, 6H), 1.04 (t, J = 7.32 Hz, 3H), 1.42 (qt, J = 7.32 Hz, 4H), 1.53–1.69 (m, 6H), 1.85 (tt, J = 6.59 Hz, 2H), 3.35 (t, J = 7.56 Hz, 4H), 4.44 (t, J = 6.59 Hz, 2H), 6.37 (d, J = 2.44 Hz, 1H), 6.60 (dd, J = 2.44, 9.03 Hz, 1H), 7.42 (dd, J = 0.96, 8.05 Hz, 1H) 7.70 (s, 1H), 7.74 (dd, J = 8.05 Hz, 1H), 7.86 (d, 9.27 Hz, 1H), 8.11 (d, J = 9.03 Hz, 1H), 8.34 (dd, J = 1.71, 9.03 Hz, 1H), 8.92 (d, J = 1.71 Hz, 1H), 8.95 (dd, J = 0.97, 7.81 Hz, 1H); elemental analysis calcd (%) for $C_{35}H_{37}N_3O_3$: C 76.75, H 6.81, N 7.76; found; C 76.74, H 6.81, N 7.62.

Compound **6b**: mp.198 °C; IR(KBr)/cm^{-1}: 1716; ^{1}H-NMR ($CDCl_3$) δ = 1.01 (t, J = 7.32 Hz, 6H), 1.03 (t, J = 7.56 Hz, 3H), 1.42 (qt, J = 7.32, 7.56 Hz, 4H), 1.52–1.69 (m, 6H), 1.83 (tt, J = 6.59 Hz, 2H), 3.43 (t, J = 7.56 Hz, 4H), 4.43 (t, J = 6.59 Hz, 2H), 6.34 (d, J = 2.44 Hz, 1H), 6.58 (dd, J = 2.44, 9.03 Hz, 1H), 7.41 (dd, J = 1.22, 8.05 Hz, 1H) 7.68 (s, 1H), 7.71 (dd, J = 8.05 Hz, 1H), 7.83 (d, 9.03 Hz, 1H), 8.22 (d, J = 8.78 Hz, 1H), 8.27 (dd, J = 1.95, 8.78 Hz, 1H), 8.82 (d, J = 1.22 Hz, 1H), 8.93 (dd, J = 1.22, 8.05 Hz, 1H); elemental analysis calcd (%) for $C_{35}H_{37}N_3O_3$: C 76.75, H 6.81, N 7.67; found; C 76.61, H 6.87, N 7.63.

4.3. Computational methods

All calculations were performed on a FUJITSU FMV-ME4/657. The semi-empirical calculations were carried out with the WinMOPAC Ver. 3 package (Fujitsu, Chiba, Japan). Geometry calculations in the ground state were carried out using the AM1 method. All geometries were completely optimized (keyword PRECISE) by the eigenvector following routine (keyword EF). Experimental absorption spectra of the symmetric phenazine derivatives were studied with the semi-empirical method INDO/S (intermediate neglect of differential overlap/spectroscopic). All INDO/S calculations were performed using single excitation full SCF/CI (self-consistent field/configuration interaction), which includes the configurations with one electron excited from any occupied orbital to any unoccupied orbital, 225 configurations were considered for the configuration interaction [keyword CI (15 15)].

4.4. X-Ray crystal structure determinations

The X-ray structure analysis was made on a Rigaku Rapid-S imaging plate (MoKα radiation, λ = 0.71069 Å, graphite-monochromator, T = 296 K, $2\theta_{max}$ = 55.0°). The structure solved by the direct method SHELXS. The non-hydrogen atoms were refined anisotropically. Hydrogene atoms were included but not refined. All calculations were performed using the SHELXL-97 package program [20]. CCDC-829423 (**3a**) contains the supplementary crystallographic data for this paper. These data can be obtained free of charge from The Cambridge Crystallographic Data Centre via www.ccdc.cam.au.uk/data_request/cif

Compound **3a**: Crystal of **3a** was recrystallized from CH_2Cl_2:AcOEt = 10:1 as red plate, air stable. The one selected had approximate dimensions 0.50 mm × 0.40 mm × 0.30 mm. The transmission factors ranged from 0.960 to 0.976. Crystal data. $C_{35}H_{37}N_3O_3$, M = 546.68, triclinic, a = 9.3372 (7), b = 12.2943 (11), c = 13.4910 (9) Å, β = 95.1518 (18)°, V = 1428.67 (19) Å^3, space group P1- (#2), Z = 2, 14093 reflections measured, 6471 unique (R_{int} = 0.0258) which were used in all calculations. The final R indices were $R1$ = 0.0710, wR (F^2) = 0.2035 (all data).

4.5. Preparation of dye-doped polymer films

Dye-doped polymer films were prepared as follows. The dye–polymer solution was firstly prepared by dissolving polymer resin pellets of PLA, PMMA, or PS (2.0 g) and the fluorescent dye (1.0 mg) in dichloromethane (10 ml). The dye–polymer solution of 0.6 ml was casted onto a cover glass (Iwaki), which was putted in a vessel saturated dichloromethane vapor for 3 h and then allowing them to dry in a vacuum oven for 24 h at 40 °C. The obtained films were found to be ca. 100 μm thickness as measured using a thickness meter (SM-1201 TECLOCK Co. LTD.). The absorption and fluorescence spectra were measured using a blank-film slide as a reference. The photofading test was carried out by using a Q-Lab Q-Sun Xe-1.

Acknowledgments

This work was partially supported by a Grant-in-Aid for Science and Research from the Ministry of Education, Science, Sport and Culture of Japan (Grant 21550181) and by a Adaptable and Seamless Technology Transfer Program through Target-driven R&D of Japan Science and Technology Agency (JST).

References

[1] N.C. Rajapaks, J.W. Kelly, J. Am. Soc. Hort. Sci. 117 (1992) 481–485.
[2] N. Noè, T. Eccher, E.D. Signore, A. Montoldi, Biol. Plant 41 (1998) 161–167.

[3] E. Oyaert, E. Volckaert, P.C. Debergh, Sci. Hort. 79 (1999) 195–205.
[4] R. Muleo, S. Molini, Sci. Hort. 108 (2006) 364–370.
[5] L. Oberhaus, J.F. Briand, C. Leboulanger, S. Jacquet, J.F. Humbert, J. Phycol. 43 (2007) 1191–1199.
[6] S. Molini, R. Muleo, in: Jain, Ishii (Eds.), Micropropagation of Woody Trees and Fruits, Kluwer Academic Publishers, Dordrecht, the Netherlands, 2003, pp. 3–35.
[7] C. D'Onofrio, S. Molini, Adv. Hort. Sci. 16 (2004) 47–52.
[8] K. Hamada, K. Shimasaki, Y. Nishimura, H. Egawa, K. Yoshida, Hort. Environ. Biotechnol. 50 (2009) 319–323.
[9] S. Hemming, E.A. van Os, J. Hemming, J.A. Dieleman, Eur. J. Hort. Sci. 71 (2006) 145.
[10] C. Kittas, A. Baille, J. Agric. Eng. Res. 71 (1998) 193.
[11] K. Hamada, K. Shimasaki, T. Ogata, Y. Nishimura, K. Nakamura, E.H. Ooyama, K. Yoshida, Environ. Control Biol. 48 (2010) 127–132.
[12] J.J.P. Stewart, Method J. Comput. Chem. 10 (1989) 209.
[13] J.E. Ridley, M.C. Zerner, Theor. Chim. Acta 32 (1973) 111.
[14] J.E. Ridley, M.C. Zerner, Theor. Chim. Acta 42 (1976) 223.
[15] A.D. Bacon, M.C. Zerner, Theor. Chim. Acta 53 (1979) 21.
[16] M. Adachi, Y. Murata, S. Nakamura, J. Org. Chem. 58 (1993) 5238–5244.
[17] W.M.F. Fabian, S. Schuppler, O.S. Wolfbesis, J. Chem. Soc. Perkin Trans. 2 (1996) 853–856.
[18] Y. Ooyama, T. Okamoto, T. Yamaguchi, T. Suzuki, A. Hayashi, K. Yoshida, Chem. Eur. J. 12 (2006) 7827.
[19] B.I. Burgess, P. Rochon, N. Cunningghham, Opt. Mater. 30 (2008) 1478–1483.
[20] G.M. Sheldrick, SHELX-97-Program for the Refinement of Crystal Structures, University of Göttingen, Germany, 1997.